Journal of Electromyography and Kinesiology 32 (2017) 101–109

Contents lists available at ScienceDirect

Journal of Electromyography and Kinesiology

journal homepage: www.elsevier.com/locate/jelekin

An EMG-driven biomechanical model of the canine cervical spine

M. Alizadeh [a,*], G.G. Knapik [a], J.S. Dufour [a], C. Zindl [b], M.J. Allen [b,c], J. Bertran [c], N. Fitzpatrick [d], W.S. Marras [a]

[a] Spine Research Institute, The Ohio State University, 520 Baker Systems, 1971 Neil Avenue., Columbus, OH 43210, USA
[b] Surgical Discovery Center, Department of Veterinary Medicine, University of Cambridge, Madingley Road, Cambridge CB3 0ES, UK
[c] Department of Veterinary Clinical Sciences, The Ohio State University, Columbus, OH 43210, USA
[d] Fitzpatrick Referrals, Eashing, Surrey GU7 2QQ, UK

ARTICLE INFO

Article history:
Received 7 June 2016
Received in revised form 23 November 2016
Accepted 22 December 2016

Keywords:
Dog
Neck
Electromyography
Dynamic
Kinematics

ABSTRACT

Due to the frequency of cervical spine injuries in canines, the purpose of this effort was to develop an EMG-driven dynamic model of the canine cervical spine to assess a biomechanical understanding that enables one to investigate the risk of neck disorders. A canine subject was recruited in this investigation in order to collect subject specific data. Reflective markers and a motion capture system were used for kinematic measurement; surface electrodes were used to record electromyography signals, and with the aid of force plate kinetics were recorded. A 3D model of the canine subject was reconstructed from an MRI dataset. Muscles lines of action were defined through a new technique with the aid of 3D white light scanner. The model performed well with a 0.73 weighted R^2 value in all three planes. The weighted average absolute error of the predicted moment was less than 10% of the external moment. The proposed model is a canine specific forward-dynamics model that precisely tracks the canine subject head and neck motion, calculates the muscle force generated from the twelve major moment producing muscles, and estimates resulting loads on specific spinal tissues.

1. Introduction

The large breed dogs are particularly susceptible to cervical spine injuries because of the large moment generated by the head relative to the base of the spine (Breit and Künzel, 2004; Crisco et al., 1990; Jeffery et al., 2013). In order to develop a better understanding of preventive strategies and effective therapeutic interventions, a more quantitative appreciation of canine cervical spine biomechanics is desirable, since a detailed biomechanical knowledge of the frequent sites of cervical spine injury is required. Biologically-assisted biomechanical models provide a viable environment to understand spine tissue loading *in vivo*. Once developed, these models are capable of helping to understand potential injury risk by accounting for how muscles are dynamically recruited and how the patterns of muscles recruitment collectively impose forces on tissues under various daily activities. It is believed that this model will significantly help to understand canine cervical spine kinematics which is still not well understood (Johnson et al., 2011). In addition, such a model can help us understand the implications of contemplated surgeries on the biomechanical behavior of the spine. Beyond the application of canine cervical spine biomechanical models in veterinary medicine, these models could be used further to better understand complex biomechanical relationships and the knowledge gained can be translated and applied to human spine models. *In vivo* studies on canines can be easily conducted and used to validate overall subject-specific model outputs. Moreover, this model will provide a suitable platform to explore the validity of canine cervical spine models that have been employed extensively for investigating effects of spinal instruments developed for human spine (Autefage et al., 2012; Lim et al., 1994; Sharir et al., 2006; Sheng et al., 2010). Several human cervical spine models have been developed and validated the human spine (Horst et al., 1997; Hyeonki Choi, 2010; Jager et al., 1996; Lopik and Acar, 2007; Snijders et al., 1991; Stemper et al., 2004; Vasavada et al., 1998), however in spite of the high frequency of spinal injuries in canines (Foss et al., 2013; Jeffery et al., 2013), attempts to develop canine cervical spine models have been lacking.

The EMG-driven biomechanical modeling approach is believed to accurately estimate spinal loads since it accounts for realistic antagonist muscle co-contraction during dynamic physical activities while account for individual variability across subjects and conditions in muscle recruitment.

* Corresponding author at: The Ohio State University, Spine Research Institute, 1971 Neil Avenue, Room 520, Columbus, OH 43210, USA.
E-mail address: Alizadeh.3@osu.edu (M. Alizadeh).

http://dx.doi.org/10.1016/j.jelekin.2016.12.008
1050-6411/

Therefore, the objective of this study was to develop a canine specific EMG-driven cervical spine model that would be sensitive to dynamic physical exertions of the cervical spine and capable of accurately predicting internal moments and spinal tissue loading profiles.

2. Methods

2.1. Modeling approach

We applied well developed human spine modeling concepts to the development of a canine cervical spine biomechanical model (Marras and Granata, 1997; Theado et al., 2007). Several experimentally measured parameters were incorporated as model inputs to predict the resultant internal moments and spinal loads as model outputs (Fig. 1). Below we briefly describe how the model inputs were acquired and implemented into the model.

2.1.1. Muscle modeling

Muscle function is represented as a three-dimensional vector function of force magnitude and force direction via dynamic muscle lines of action. Dynamic tensile force of a muscle (j) is estimated (Eq. (1)) as the product of muscle gain ratio ($GainRatio_j$), EMG (EMG_j), muscle cross-section area ($Area_j$), while taking into account the force-length ($f(L_j(t))$) and force-velocity ($f(V_j(t))$) relationship of the muscles (Theado et al., 2007). Raw EMG signals processing are described in detail by (Dufour et al., 2013). Moment generated by the muscles (M) were calculated via summation of vector products between muscle (j) tensile force (F) and its moment arm (r) at every time point during the dynamic trial (Eq. (2)) (Theado et al., 2007).

Muscle moment arm is defined as the perpendicular distance of muscle line of action from the joint axis of rotation (Vasavada et al., 1998). The model is operating such that the gain ratio for each muscle was predicted within a calibration trial, in order to personalize muscle forces for the canine subject similar to the technique that was developed by Dufour et al. (2013) for human lumbar spine muscles. Once these parameters for each muscle were specified, they were applied to analyze collected trials performed by the canine subject. In order to accurately estimate muscle gain ratio, an optimization algorithm had been used to minimize error between muscles' internal moments and external moments about cervical spine joints. Based on the anatomical properties of muscles in this model, the objective function of calibration algorithm aimed to minimize moment prediction errors in two joints, C1/C2 and C7/T1. The boundary conditions for the calibration procedure used here were originally developed for the human lumbar spine. However, previous studies have shown relatively similar muscle parameters between humans and canines (McCully and Faulkner, 1983).

$$F_j(t) = GainRatio_j \cdot Area_j \cdot EMG_j(t) \cdot f[L_j(t)].f[V_j(t)] \quad (1)$$

$$\overrightarrow{M} = \sum_{j=1}^{10} \vec{r}_j(t) \times \vec{F}_j(t) \quad (2)$$

Due to the lack of comprehensive canine neck muscle properties to approximate muscle lines of action and cross-sectional areas, the best technique for determining these parameters for this model had to be investigated. Medical imaging techniques like magnetic resonance imaging (MRI) and cadaveric experiments are two of the most well established methods to measure muscle moment arms and to define muscle line of action (Borst et al., 2011; Dumas et al., 1991; Macintosh and Bogduk, 1991; Németh and Ohlsén, 1986). However there are many sources of inaccuracies associated with these techniques. First, and the most probable shortcoming was that of the partial volume effect phenomena, where a large bias can be introduced in measured parameters on medical images (Soret et al., 2007). Second, scan planes are generally perpendicular to the scan table while the direction of the muscles are most probably oblique to the scan plane, consequently cross-sectional areas (CSA) derived from images are typically overestimated (Jorgensen et al., 2003). Adjusting the CSA for muscle fiber angle can reduce this error, however, muscle fiber directions are often not detectable via MRI. Considering individual variability

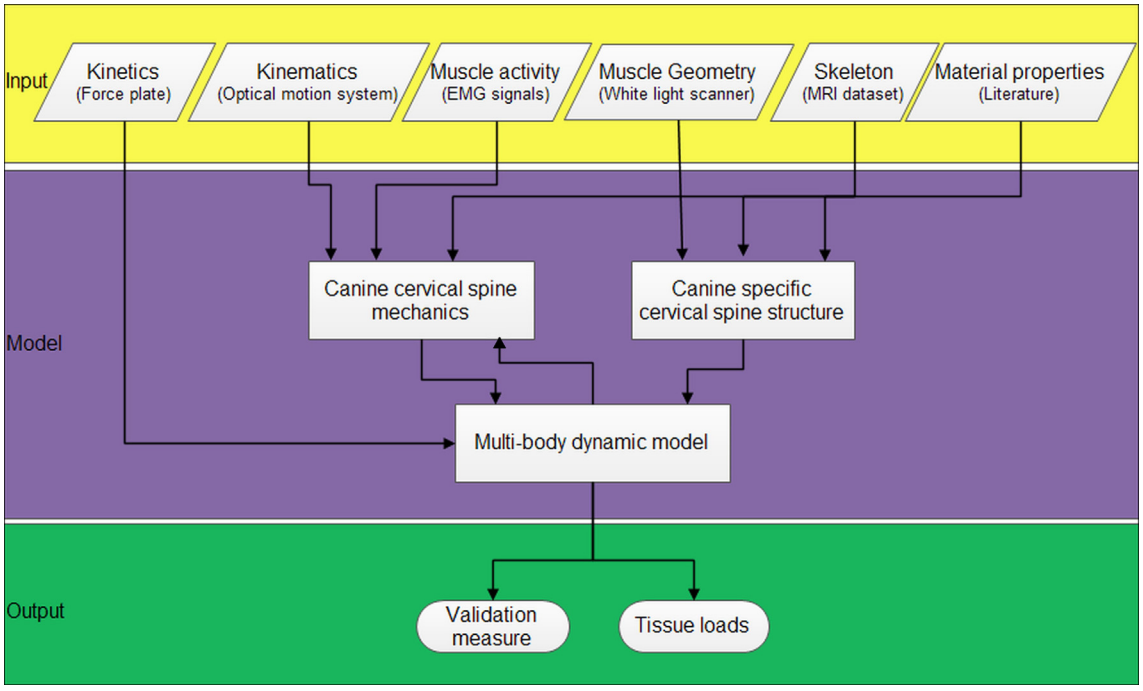

Fig. 1. Display of the overall modeling logic.

across subjects, it is impossible to correct CSA for the subject-specific models with medical images. Third, distinguishing muscles and separating them from one another requires a thorough knowledge of cross-sectional anatomy as well as powerful MRI imaging to be able to visually differentiate muscles. In order to reduce error introduced by these limitations in the model, an alternative approach was investigated to determine muscle line of action.

The application of a three-dimensional white light scanner (3DWLS) (Artec Eva, Artec, Palo Alto, CA, USA) to determine muscle lines of action while minimizing medical imaging shortcomings was investigated. The Artec Eva 3D scanner consists of a portable camera that dynamically captures 3D geometry data and surface information at up to 15 Hz. It is an ideal tool for medical scanning purposes because: (a) the 3D scanner is able to provide a 3D view of an object to help identify cervical spine muscles in their complex geometrical arrangement; and, (b) the scanner is capable of providing high resolution images while capturing texture at high speed. One advantage of this approach is that measurements such as fiber angles and muscle cross-sections are taken directly from intact muscles without disturbing muscle attachments. Therefore, more accurate measurements in comparison to previous direct dissection cadaveric studies would be expected. A cadaver dog, similar to the subject, euthanized for another research protocol unrelated to this study was used to test the proposed technique for determining canine cervical muscle lines of action.

The dog specimen dissection process started by removing the skin and underlying subcutaneous fat and connective tissue until the superficial muscle was exposed in the neck region. Then, the 3DWLS was used to scan the exposed muscle. Next, every single muscle in the neck region was removed carefully one at a time, and the 3DWLS was used to capture the surface information of the next layer of exposed intact muscle. Within post processing muscle volume was then defined as a volume between two consecutive scans obtained in the order as described previously. Each muscle's line of action was then approximated by the three dimensional centroid path of that muscle (Jaeger et al., 2011). Finally, to reduce modeling complexity a straight line was fitted to the centroid path obtained by multiple planes (Jaeger et al., 2011) and further used as the straight muscle line of action.

Among the many muscles in the neck, six muscle pairs were chosen based on their moment arm length, their cross-sectional area, and their accessibility via surface electromyography electrodes. These twelve muscles were: left/right sternomastoid, left/right obliquus capitis, left/right splenius, left/right biventer, left/right complexus, and left/right longissimus. Anatomically, the splenius muscle is located dorsal to the biventer and complexus muscles, with a larger cross-sectional area and moment arm. This indicated that more activation was expected to be seen from the splenius than the biventer and complexus muscles. Considering the capability of surface electrodes on detecting different signals, it was not practical to locate separate electrodes for the splenius, biventer and complexus muscles. Therefore, we recorded splenius activity by EMG electrodes and we assumed the same recruitment pattern shape would apply to the biventer and complexus muscles.

2.1.2. Geometry reconstruction

In order to generate the subject-specific anatomical model, the canine subject underwent MRI imaging. A series of image post-processing operations were performed on the MRI images in order to obtain a detailed three-dimensional model of the canine cervical spine (Skull - T1).

2.1.3. Ligaments and intervertebral disc modeling

Ligaments were modeled as passive force vectors located between two points representing ligament attachment points (Kumar, 2012). The nuchal ligament, dorsal atlanto-occipital membrane, lateral atlanto-occipital membrane, dorsal atlanto-axial ligament, ventral atlanto-axial membrane, alar ligament, transverse atlantal ligament, apical ligament, alar ligament, apical ligament, ventral longitudinal ligament, dorsal longitudinal ligament, yellow ligament, interspinous ligament, and capsular ligament were all incorporated in the model. The width of the ligament was represented using multi force vectors to ensure that the force could encompass the complete physiological width of the ligament. Due to lack of canine ligament properties, human cervical spine ligament properties were used in the model instead (Han et al., 2012). Intervertebral discs geometry at each cervical spine level was reconstructed from the MRI dataset and its material properties obtained from the literature (Zimmerman et al., 1992). The intervertebral discs were modeled as three dimensional spring dampers located at the center of the disc space for each motion segment. Therefore, at each spinal joint there is an intervertebral disc and anatomically matched ligaments in order to stabilize the joint. The atlanto-occipital and atlanto-axial joints are two complex joints with a shared common joint capsule. Cartilage at these joints was modeled as three dimensional spring dampers with stiffness properties similar to cartilage stiffness (Jaumard et al., 2011). The final 3D dynamic model of canine cervical spine is shown in Fig. 2.

2.2. Modeling approach

2.2.1. Experimental tasks and training

A skeletally mature male hound (26.0 kg body weight) served as the subject in this study. The dog was examined by a veterinarian and documented to be healthy, with no evidence of joint or spinal

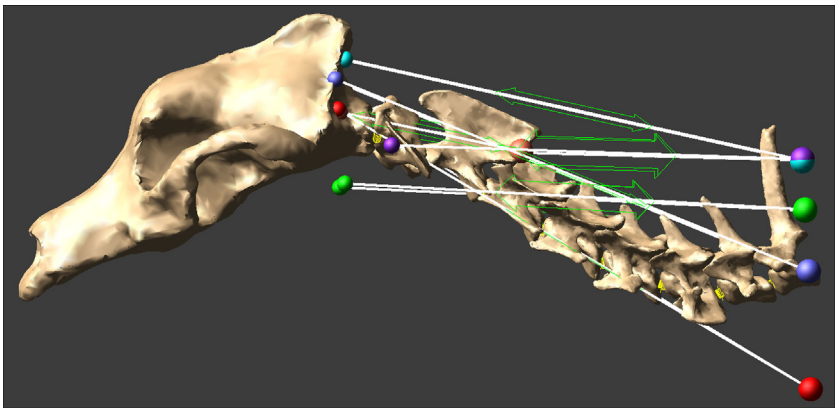

Fig. 2. Dynamic model of the canine cervical spine with straight line muscles. ● longissimus, ● complexus, ● sternocleidomastoid, ● splenius, ● obliquus capitis, ● biventer.

disease. The dog was housed in a room with other dogs and was fed a standard laboratory dog chow with water *ad libitum*. During three weeks before data collection, the dog was trained using food treats to allow for passive manipulation of the head and neck via a soft head collar (Gentle Leader, Suffolk, UK). Beginning from the neutral position, various exertion trials ranging from simple deep flexion/extension to more complex exertions including axial rotation and lateral bending were performed. Movements were repeated with the head and neck turning from the left to the right side and for motion of the head and neck in trajectory of oblique flexion and extension. After going through all motion sequences, a latex resistance band (TheraBand, Akron, OH, USA) was attached to the head collar at the mandibular part of the collar. The opposite end of the resistance band was manually held with the hand placed in a fixed position on the floor and the resistance band perpendicular to the floor, so that no traction was applied to the resistance band when the head was in neutral position. The sequence of passive head/neck movements was then repeated with the resistance band in place. In order to slowly acclimate the dog to the resistance, training during the first week was carried out with a band of medium resistance and during subsequent training sessions (week 2 and 3) and at the testing day with a band of higher resistance.

2.2.2. Subject

The experimental procedures for this study were reviewed and approved by the local institutional animal care and use committee (IACUC). During the experiment, the dog was encouraged to follow food treats to resemble the training procedure. The resistance band in the experimental trial was not manually held, but fixed on the force plate on ground level (Fig. 3).

2.2.3. Data collection system (Apparatus)

Bipolar surface electrodes were placed over 8 neck muscles (four pairs of muscles). EMG data was collected with a MA300-XVI Advanced Multi-channel EMG System (Motion Lab Systems Incorporated, Baton Rouge, Louisiana, USA) at 1000 HZ collection frequency. The latex resistance band force and moment were measured via a force plate (Bertec 4060A; Bertec, Worthington, OH, USA). An OptiTrack optical motion capture system (NaturalPoint, Corvallis, OR, USA) with 24 Flex 3 infrared cameras was used to capture optical marker locations during the experiment via OptiTrack's Motive software. Custom software developed at the Ohio State University Spine Research Institute was used to record analog signals through a NI USB-6225 Data Acquisition Device (National Instruments, Austin, TX, USA) and to control and sync optical data collection.

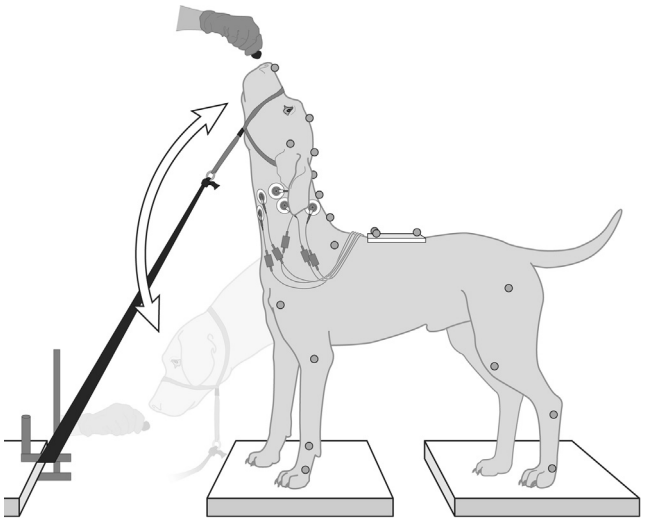

Fig. 3. Trial set up: the subject is placed on two force plates, the latex resistance band (TheraBand, Akron, OH, USA) is connected to the neck of the mandibular part of the soft head collar on one end and to the force plate from the other end. The subject was naturally with its own intention pulling against the latex resistance band in order to eat the food treat.

2.2.4. Kinematic and kinetic data acquisition

Three reflective markers (optical) were attached to the bony landmarks of the head: (1) left frontal process, (2) right temporozygomatic bone, and (3) left nasal bone. Three more markers were attached to a small solid panel made of plastic that was tightly secured to the back of the dog to serve as a rigid body. Three more reflective markers were glued to the neck in the areas of the spinous processes of C2, C5 and C7 and two additional markers were placed on the spine of the scapula to represent shoulder movement (Fig. 4). The optical marker locations were recorded during each trial by the motion capture system. Optical marker position data was then used to calculate the kinematics of the head, neck and back. Developing a multi-segmental model allowed us to define angular displacement for each joint based on the data recorded by the motion capture system.

Force and moment data from the force plate and inertial moment contributions of the head and vertebral bodies together, were served to define the total external moment.

2.2.4.1. Muscle EMG data acquisition. EMG activities of the four pairs of extensor/flexor neck muscles were recoded using surface electrodes. The investigated muscles were: left/right obliquus capitis, left/right splenius, left/right longissimus, and left/right sternocleidomastoid (Fig. 5). These muscles were chosen since they are all major power producing neck muscles based on their cross-section area, and functionality. The EMG electrodes were located on shaved, cleaned and alcohol treated skin based upon a study of the anatomical description of muscle locations (Alizadeh et al., submitted for publication). The skin preparation was similar to previously published paper (Marras and Davis, 2001).

MRI imaging was scheduled after the experimental part in order to precisely document the anatomical features of the vertebral bodies. T1 and T2 weighted MRI images were acquired on a 3T MRI scanner (Magnetom Trio, Siemens Healthcare, Erlangen, Germany). Transverse slices of 1 mm thickness were obtained from the skull level and extended caudally to the level of the second thoracic vertebra. This imaging session was also used to validate the EMG electrode and optical marker location. The locations of the EMG electrodes were indicated with diagnostic MRI markers. These markers showed up well in the imaging allowing each electrode to be paired with the correct target muscle. In addition, custom made dual modality markers were used to line up optical motion capture data with the MRI data. These consisted of diagnostic MRI markers embedded within optical motion capture markers (Fig. 6).

3. Results

3.1. Validation

Based on the findings of Dufour et al. (2013), the acceptable range for gain ratio of 6–131 N/cm^2 V was adopted to represent the physiological acceptable range of gain in humans (Granata and Marras, 1993). The gain ratio for each muscle calculated in this study was between 30 and 80, which fell within the predicted physiological range previously reported for human spine.

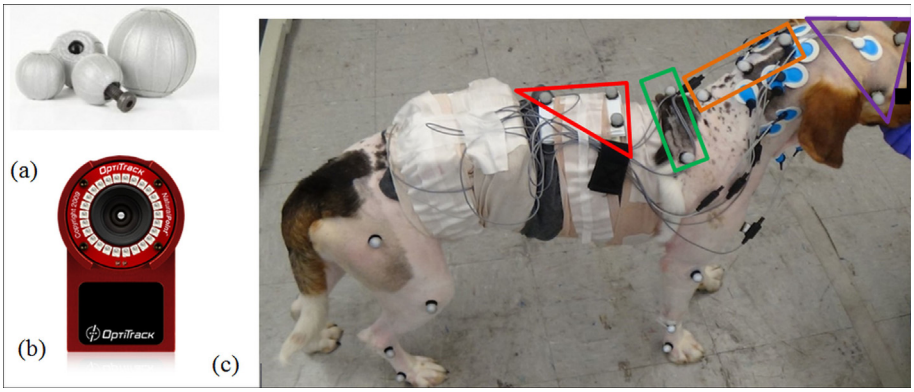

Fig. 4. Kinematic data collection: (a) Reflective optical markers. (b) Optical motion capture camera. (c) Location of reflective optical markers in order to measure joint angles: Head markers, Neck markers, Shoulder markers, UpperTorso markers.

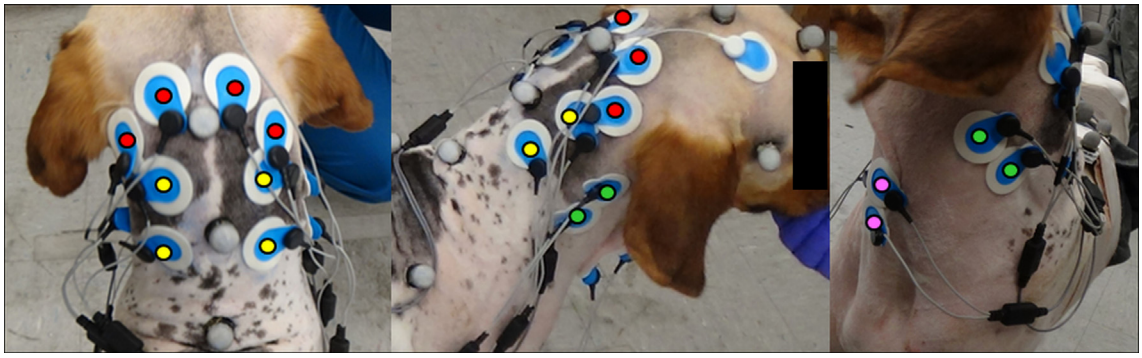

Fig. 5. Surface electromyography (EMG) electrode location, Obliquus capitis, Splenius, Longissimus, Sternocleidomastoideus.

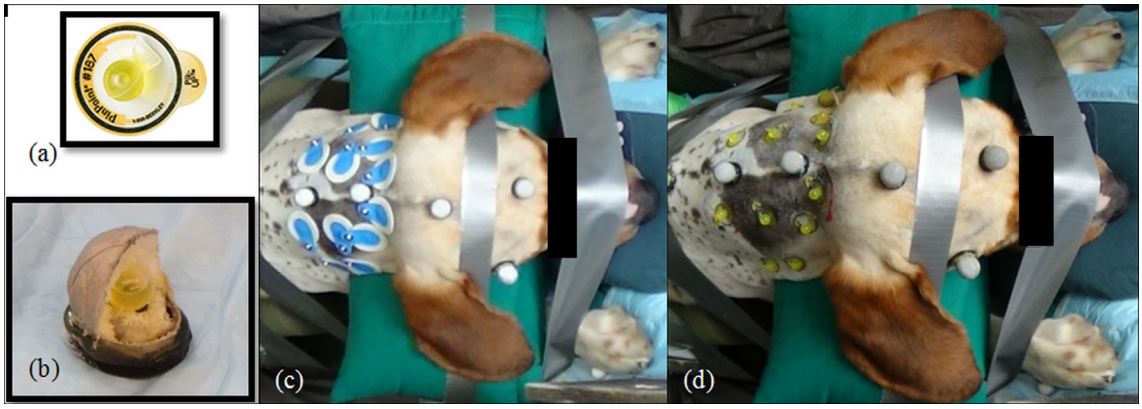

Fig. 6. (a) MRI diagnostic marker, (b) dual modality marker (cut in half for clarity), replacing reflective optical markers, (c) location of EMG electrodes and dual modality markers, (d) replaced EMG electrodes with MRI diagnostic marker.

The reliability of the model was investigated by comparing the measured resultant dynamic external moment to the predicted internal moment produced by the muscles and ligaments in both the sagittal and axial planes via their correlation coefficient (R^2) and average absolute error (AAE). Comparison of the measured external moment and the predicted internal moment (over time) is illustrated in Fig. 7. The model performed well with a 0.73 weighted R^2 value in multiple planes, considering each plane contribution in generated moment. The weighted average absolute error of the predicted moment was less than 10% of the external moment in the calibration trial.

3.2. Spinal load

Fig. 8 shows the peak spinal load at all the levels during the trial. The injury force tolerance threshold for canine cervical spine has not been defined. Therefore, we will only comment on the spine loading pattern in a relative fashion. Compression forces gradually increased from C1/C2 to C4/C5 where they were the greatest then these forces gradually decreased toward C7/T1. The anterior/posterior (A/P) and lateral (Lat) forces varied along the length of the cervical spine.

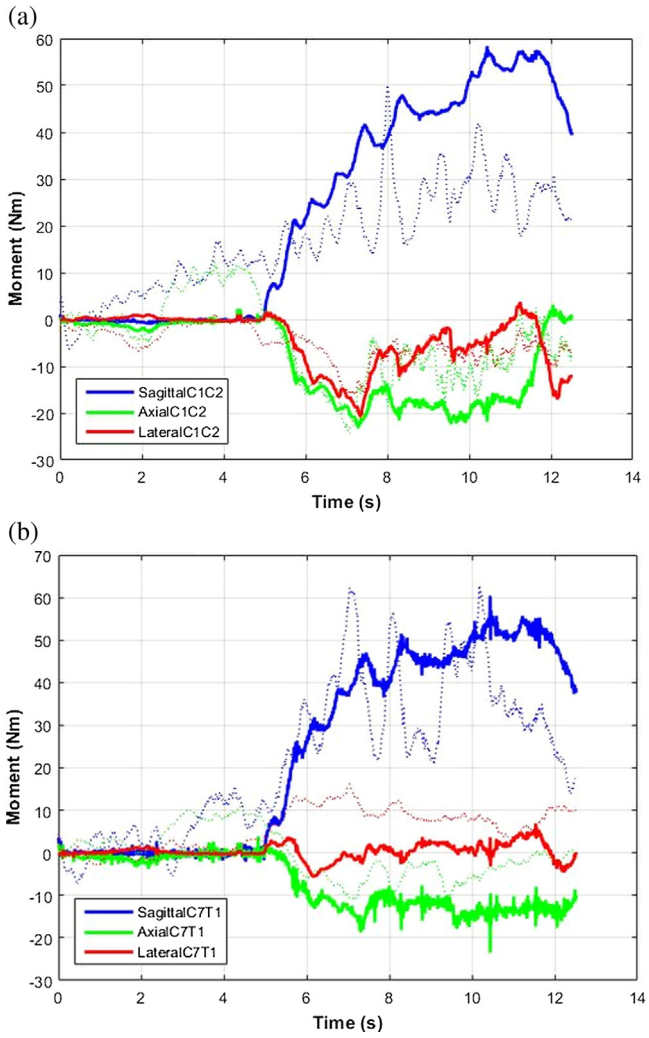

Fig. 7. Canine cervical spine measured external moments (solid lines) as a function of time during a typical exertion and the moments predicted from the EMG-assisted model for the calibration trial (dashed lines). (a) C1C2 level. (b) C7T1 level. blue = sagittal plane, green = axial plane, red = lateral plane. (For interpretation of the references to colour in this figure legend, the reader is referred to the web version of this article.)

4. Discussion

For the first time, we have been able to develop a dog-specific cervical spine biomechanical model that helps us understand the pattern of 3D moments and forces imposed upon the vertebral tissues of the spine during a complex dynamic exertion made by a live animal.

The compression spine loads indicated a reasonable and expected pattern of loading, where the highest compression values occurred at the C4/C5 level, similar to that reported by Yoganandan et al. (2001) in the human cervical spine. It is not advisable to validate model fidelity by quantifying spinal loads magnitude, since there is no experimental data on canine cervical spine failure threshold to our knowledge. Moreover, due to the significant differences between human and canine cervical spine ranging from tissue material properties to postural variation and type of physical activities they are exposed to, it is not reasonable to compare them. A similar argument can be made for the muscle forces and moments. One might consider the magnitude of internal moments and spinal loads observed during the trial (Fig. 8) to be very large. However, when considering the fact that the dog was pulling forcefully against a strong latex resistance band, these spine loading magnitudes are not out of the range of possibilities in the exertions may be close to a maximum exertion for the animal.

The current EMG-driven dynamic model is unique in that it was dog specific in terms of: (1) muscle morphometric properties such as CSA, (2) muscle line of action, (3) muscle activities, and (4) subject kinematics. The model structure is multi-dimensional and is capable of considering dynamic responses of the subject.

This model is advanced in many aspects which two of them are outstanding. First, this is a multi-segmental cervical spine model in which motion segments between the skull and T1 are separated and are allowed to move relative to each other. The advantage of the multi-segmental cervical spine can be emphasized at the atlanto-occipital and atlanto-axial joints. According to Dugailly et al.,(2011), 40% of axial rotation occurs at the atlanto-axial joint, with the rest being distributed along the rest of the neck. This allowed us to define angular displacement for each joint based on the data recorded by the motion capture system. As a result, the error introduced into the model by implementing the calculated joint angles from the recorded data of motion capture system was less than 0.5 mm. Therefore, the model motion was very similar to the actual dog motion. It is believed that while the joint kinematics are precisely defined in the model, muscle moment

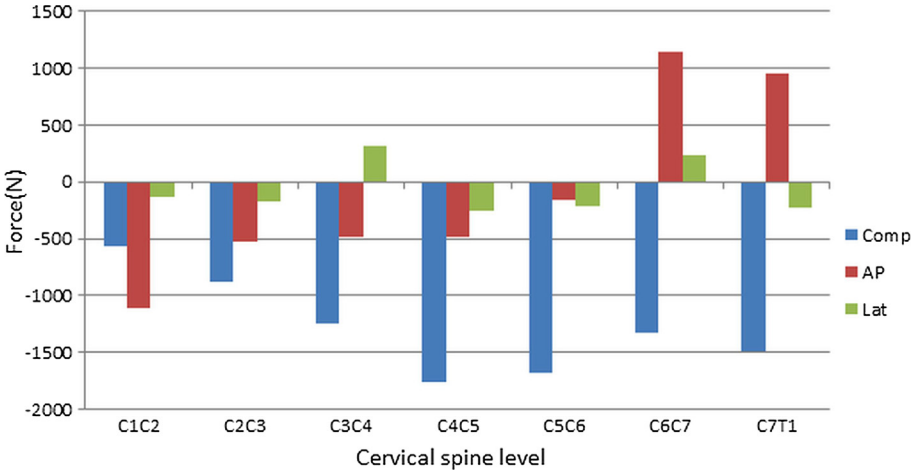

Fig. 8. Maximum spinal loads (N) measured during the trial at each cervical spine level (comp = compression, AP = anterior-posterior shear, Lat = lateral shear).

arm and consequently measured internal moment at each time point during the trial will be estimated more accurately.

Second, the muscle lines of action were determined in a cadaver-based experiment with a precise technique. The advantages of this technique in comparison to the previously established cadaver experiments were: (1) muscle measurements such as cross-sectional area were achieved without disturbing muscle attachments, (2) muscle CSA could be measured at any level, and (3) estimated muscle lines of action were represented realistically since they were fitted to the muscle centroid curve created by connecting muscle centroids in various planes, corrected for muscle fibers angle.

As with any assessment tool one must appreciate the limitations of the model. First, it should be noted that this model was developed based on data from a single animal subject. Therefore, the estimated muscle properties including initial muscle length, CSA, and muscle line of action are unique to this animal and are not necessarily representative of all canines. Another limitation associated with the performance of the model is that at the beginning of the trial a strong correlation between the predicted and measured moments were not observed. However, one must consider that during the first quarter of the trial, the dog was not pulling against the latex band due to the flexed posture of the neck. Thus, measured external moments for this portion of the task were negligible, while internal moments were registered from the muscles. This discrepancy may be due to limitations in the way inertial characteristics were estimated for the head and vertebrae. Better approximations for these unknown variables will need to be determined in the future. In addition, there were several parameters in the model that had been taken from a well-established human spine model. Further investigation is necessary to determine more representative parameters for canines.

5. Conclusions

We believe the presented model is an important achievement in terms of application of engineering principals to veterinary medicine and a significant step forward to understand canine cervical spine biomechanics. The model met the objectives well by being able to track the motion precisely, accurately predict internal moments of cervical spine based on the measured external moments, and estimate spinal tissue loads that are reasonable based on the task that was performed. Such an advanced canine specific model could be eventually used routinely by veterinary orthopedic and rehabilitation centers to evaluate treatment strategies and surgical techniques before applying them on the canine patient.

Conflict of interest

None declared.

Acknowledgements

This work was supported in part by Fitzpatrick Referrals Ltd., through the One Health/One Medicine Fellowship at The Ohio State University. The authors thank Tim Vojt (College of Veterinary Medicine) for preparing the original artwork for this paper.

References

Alizadeh, M., Zindl, C., Allen, M.J., Knapik, G.G., Fitzpatrick, N., Marras, W.S., 2016. MRI Cross sectional atlas of normal canine cervical musculoskeletal structure. Res. Vet. Sci. 109, 94–100.

Autefage, A., Palierne, S., Charron, C., Swider, P., 2012. Effective mechanical properties of diaphyseal cortical bone in the canine femur. Vet. J. Lond. Engl. 1997 (194), 202–209.

Borst, J., Forbes, P.A., Happee, R., Veeger, D., 2011. Muscle parameters for musculoskeletal modelling of the human neck. Clin. Biomech. 26, 343–351.

Breit, S., Künzel, W., 2004. A morphometric investigation on breed-specific features affecting sagittal rotational and lateral bending mobility in the canine cervical spine (C3–C7). Anat. Histol. Embryol. 33, 244–250.

Crisco, J.J., Panjabi, M.M., Wang, E., Price, M.A., Pelker, R.R., 1990. The injured canine cervical spine after six months of healing. An in vitro three-dimensional study. Spine 15, 1047–1052.

Dufour, J.S., Marras, W.S., Knapik, G.G., 2013. An EMG-assisted model calibration technique that does not require MVCs. J. Electromyogr. Kinesiol. Off. J. Int. Soc. Electrophysiol. Kinesiol. 23, 608–613.

Dugailly, P.-M., Sobczak, S., Moiseev, F., Sholukha, V., Salvia, P., Feipel, V., Rooze, M., Van Sint Jan, S., 2011. Musculoskeletal modeling of the suboccipital spine: kinematics analysis, muscle lengths, and muscle moment arms during axial rotation and flexion extension. Spine 36, E413–422.

Dumas, G.A., Poulin, M.J., Roy, B., Gagnon, M., Jovanovic, M., 1991. Orientation and moment arms of some trunk muscles. Spine 16, 293–303.

Foss, K., da Costa, R.C., Moore, S., 2013. Three-dimensional kinematic gait analysis of Doberman Pinschers with and without cervical spondylomyelopathy. J. Vet. Int. Med. Am. Coll. Vet. Intern. Med. 27, 112–119.

Granata, K.P., Marras, W.S., 1993. An EMG-assisted model of loads on the lumbar spine during asymmetric trunk extensions. J. Biomech. 26, 1429–1438.

Han, I.S., Kim, Y.E., Jung, S., 2012. Finite element modeling of the human cervical spinal column: role of the uncovertebral joint. J. Mech. Sci. Technol. 26, 1857–1864.

Horst, M.J. van der, Thunnissen, J.G.M., Happee, R., Haaster, R.M.H.P. van, Wismans, J.S.H.M., 1997. The influence of muscle activity on head-neck response during impact (SAE Technical Paper No. 973346). SAE Technical Paper, Warrendale, PA.

Hyeonki Choi RVJ. Comparison of Biomechanical Human Neck Models: Muscle Forces and Spinal Loads at C4/5 Level [WWW Document]. Hum. Kinet. J. URL <http://journals.humankinetics.com/jab-back-issues/jabvolume15issue2may/comparison-of-biomechanical-human-neck-models-muscle-forces-and-spinal-loads-at-c45-level>; 2010 [accessed 12.17.15].

Jaeger, R., Mauch, F., Markert, B., 2011. The muscle line of action in current models of the human cervical spine: a comparison with in vivo MRI data. Comput. Methods Biomech. Biomed. Eng. 15, 953–961.

Jager, M. de, Sauren A, Thunnissen J, Wismans J. A global and a detailed mathematical model for head-neck dynamics. In: Proceeding Thw 30th Stapp Car Crash Conf. SAE Paper No. 962430; 1996. p. 269–81.

Jaumard, N.V., Welch, W.C., Winkelstein, B.A., 2011. Spinal facet joint biomechanics and mechanotransduction in normal, injury and degenerative conditions. J. Biomech. Eng. 133, 071010.1–071010.31.

Jeffery, N.d., Levine, J.m., Olby, N.j., Stein, V.m., 2013. Intervertebral disk degeneration in dogs: consequences, diagnosis, treatment, and future directions. J. Vet. Int. Med. 27, 1318–1333.

Johnson, J.A., da Costa, R.C., Bhattacharya, S., Goel, V., Allen, M.J., 2011. Kinematic motion patterns of the cranial and caudal canine cervical spine. Vet. Surg. VS 40, 720–727.

Jorgensen, M.J., Marras, W.S., Gupta, P., 2003. Cross-sectional area of the lumbar back muscles as a function of torso flexion. Clin. Biomech. Bristol. Avon. 18, 280–286.

Kumar, M.S.A., 2012. Clinically Oriented Anatomy of the Dog and Cat. Linus Publications, Ronkonkoma, NY, p. 11779.

Lim, T.H., Goel, V.K., Weinstein, J.N., Kong, W., 1994. Stress analysis of a canine spinal motion segment using the finite element technique. J. Biomech. 27, 1259–1269.

Lopik, D.W. van, Acar, M., 2007. Development of a multi-body computational model of human head and neck. Proc. Inst. Mech. Eng. Part K J. Multi-Body Dyn. 221.

Macintosh, J.E., Bogduk, N., 1991. The attachments of the lumbar erector spinae. Spine 16, 783–792.

Marras, W.S., Davis, K.G., 2001. A non-MVC EMG normalization technique for the trunk musculature: Part 1. Method development. J. Electromyogr. Kinesiol. Off. J. Int. Soc. Electrophysiol. Kinesiol. 11, 1–9.

Marras, W.S., Granata, K.P., 1997. The development of an EMG-assisted model to assess spine loading during whole-body free-dynamic lifting. J. Electromyogr. Kinesiol. Off. J. Int. Soc. Electrophysiol. Kinesiol. 7, 259–268.

McCully, K.K., Faulkner, J.A., 1983. Length-tension relationship of mammalian diaphragm muscles. J. Appl. Physiol. 54, 1681–1686.

Németh, G., Ohlsén, H., 1986. Moment arm lengths of trunk muscles to the lumbosacral joint obtained in vivo with computed tomography. Spine 11, 158–160.

Sharir, A., Milgram, J., Shahar, R., 2006. Structural and functional anatomy of the neck musculature of the dog (Canis familiaris). J. Anat. 208, 331–351.

Sheng, S.-R., Wang, X.-Y., Xu, H.-Z., Zhu, G.-Q., Zhou, Y.-F., 2010. Anatomy of large animal spines and its comparison to the human spine: a systematic review. Eur. Spine J. Off. Publ. Eur. Spine Soc. Eur. Spinal Deform. Soc. Eur. Sect. Cerv. Spine Res. Soc. 19, 46–56.

Snijders, C.J., Hoek van Dijke, G.A., Roosch, E.R., 1991. A biomechanical model for the analysis of the cervical spine in static postures. J. Biomech. 24, 783–792.

Soret, M., Bacharach, S.L., Buvat, I., 2007. Partial-volume effect in PET tumor imaging. J. Nucl. Med. Off. Publ. Soc. Nucl. Med. 48, 932–945.

Stemper, B.D., Yoganandan, N., Pintar, F.A., 2004. Validation of a head-neck computer model for whiplash simulation. Med. Biol. Eng. Comput. 42, 333–338.

Theado, E.W., Knapik, G.G., Marras, W.S., 2007. Modification of an EMG-assisted biomechanical model for pushing and pulling. Int. J. Ind. Ergon. Musculoskeletal Load of Push-Pull Tasks 37, 825–831.

Vasavada, A.N., Li, S., Delp, S.L., 1998. Influence of muscle morphometry and moment arms on the moment-generating capacity of human neck muscles. Spine 23, 412–422.
Yoganandan, N., Kumaresan, S., Pintar, A.A., 2001. Biomechanics of the cervical spine Part 2. Cervical spine soft tissue responses and biomechanical modeling. Clin. Biomech. 16, 1–27.
Zimmerman, M.C., Vuono-Hawkins, M., Parsons, J.R., Carter, F.M., Gutteling, E., Lee, C.K., Langrana, N.A., 1992. The mechanical properties of the canine lumbar disc and motion segment. Spine 17, 213–220.

Mina Alizadeh is a Ph.D. student and research associate with the Spine Research Institute at The Ohio State University. She received her M.S. in Mechanical Engineering with the concentration in spine biomechanics, lumbar spine instrumentation and fixation techniques and advanced finite element modeling. Her research focuses on development and utilization of dynamic EMG-assisted biomechanical models.

Greg G. Knapik is a Senior Researcher and the Director of Computational Modeling at the Spine Research Institute. His research focuses on advanced dynamic biomechanical model development and simulation, and applied ergonomic and biomechanical studies. He specializes in human data acquisition, multi-body dynamic simulations, biomedical imaging based model development, finite element modeling, and advanced numerical methods.

Jonathan S. Dufour is an Associate Research Engineer with The Ohio State University Spine Research Institute. He received his B.S. and M.S. in Mechanical Engineering at The Ohio State University with a concentration in biomechanics. His research focuses on the development and efficient utilization of dynamic biomechanical models with an interest in technology and research commercialization.

Claudia Zindl is currently a first year resident in small animal surgery at the Department of Veterinary Medicine, University of Cambridge. She has worked as a research fellow in the Surgical Discovery Centre, Department of Veterinary Medicine, University of Cambridge and before that in the Department of Veterinary Clinical Sciences, The Ohio University, performing biomechanical studies of new implant systems for the canine cervical and lumbosacral spine, retrieval analysis studies of canine cervical disc replacement implants and several orthopaedic related clinical studies in research dogs and rabbits. Before coming to the USA she spent one year as a surgical intern at Fitzpatrick Referrals, Eashing, UK, after having worked 5 years as a small animal veterinarian in referral practices and 4 years in a mixed practice in Germany. She did her Master's thesis at the St. Louis Zoo, St. Louis, Missouri, USA improving the freezing capabilities of Mexican wolf (Canis lupus baileyi) semen after having graduated as a veterinarian in 2000 from the Stiftung Tieraerztliche Hochschule Hannover.

Matthew J Allen after initial veterinary training at the University of Cambridge, he pursued a PhD (Cambridge) and then a post-doctoral fellowship (Purdue) in comparative orthopaedics. He moved to SUNY Upstate Medical University in Syracuse, where he held joint appointments in the Departments of Orthopedic Surgery, Neuroscience & Physiology, and Laboratory Animal Resources. He was recruited to The Ohio State University in March 2008 and directed the Surgical Research Laboratory at the OSU College of Veterinary Medicine. Over my time at OSU, he established a clinical total knee replacement program in the Veterinary Medical Centre. In 2014, he was elected Professor of Small Animal Surgery at the University of Cambridge. His current research, performed in the newly established Surgical Discovery Centre, involves a mixture of preclinical and clinical research in the areas of total joint replacement, spine surgery, image-guided surgery and surgical oncology.

Judith Bertran has completed a small animal surgery residency and is currently enrolled as a fellow for surgical oncology in small animal at the Department of Veterinary Clinical Sciences, The Ohio State University. She also received her master in Comparative and Veterinary Medicine, with specific work in robotic kinematics of canine total knee replacement. Her research has focused on kinematic assessment of the canine total knee replacement as well as other orthopaedic implant performances in the small animal orthopaedic sciences. Due to her current position as a surgical oncology fellow, she is seeking opportunities to investigate the performance of different type of limb sparing procedures for limb salvage in small animals.

Prof Noel Fitzpatrick is an RCVS Specialist in Small Animal Surgery (Orthopaedics) and a Diplomate of the American College of Veterinary Sports Medicine and Rehabilitation. He is director and chief clinician in the UK's largest dedicated small animal orthopaedic and neurology facility, Fitzpatrick Referrals. He is also the Director of the Fitzpatrick Sports Medicine and Rehabilitation Centre and the biomedical engineering company Fitzbionics. He has also founded the Fitzpatrick Referrals Oncology and Soft Tissue Surgery Centre for companion animals. He has published more than fifty papers in peer-reviewed journals and has developed more than thirty new techniques and implants in orthopaedics and neuro-surgery, primarily in the fields of joint and disc replacement and limb prosthetics. He has received the Mark S Bloomberg and Simon Awards for teaching and contribution to veterinary surgery and has delivered more than one thousand lectures nationally and internationally. He has sponsored and mentored more than one hundred fellowships, internships, residencies and PhDs and is the first Professor of Orthopaedics at the University of Surrey School of veterinary medicine. His passion remains firmly anchored in the promotion of One Medicine, and he has founded The Humanimal Trust as a registered charity to fund medical research that will symbiotically benefit both animals and humans. He continues to make TV documentaries which are broadcast internationally and explore the importance of the human-animal bond in society in conjunction with our moral responsibility for animals in the context of advanced healthcare. He is the founder of The VET Festival and ONE Live, the first festival events of education and music in support of animals globally, from the perspective of promoting a fair deal for animals in medical research, co-operation between human and veterinary researchers and care providers and also advocacy for the preservation of habitats and biodiversity.

William S. Marras holds the Honda Chair in the Department of Integrated Systems Engineering at the Ohio State University. He serves as the Director of the Spine Research Institute. Professor Marras also serves as Executive Director for the Institute for Ergonomics. Dr. Marras holds joint academic appointments in the Department of Orthopaedic Surgery, the Department of Neurosurgery, and the Department of Physical Medicine & Rehabilitation. His research is centered on understanding multidimensional causal pathways for spine disorders through quantitative epidemiologic evaluations, laboratory biomechanical studies, personalized mathematical modeling, and clinical studies of the lumbar and cervical spine. His findings have been published in over 200 peer-reviewed journal articles, hundereds of refereed proceedings, and numerous books and book chapters including a book entitled "The Working Back: A Systems View". He holds Fellow status in six professional societies including the American Society for the Advancement of Science (AAAS) and has been widely recognized for his contributions through numerous national and international awards including two Volvo Awards for Low Back Pain Research and an honorary Sc.D. degree. Professor Marras has been active in the National Research Council (NRC) having served on over a dozen boards and committees and has served as Chair of the Board on Human Systems Integration for multiple terms. He has also served as Editor-in-Chief of Human Factors and is currently Deputy Editor of Spine. Professor Marras has been elected President of the Human Factors and Ergonomics Society (the world's largest such society). Dr. Marras was elected to the National Academy of Engineering (the National Academies of Science, Engineering and Medicine), recorded a TEDx talk entitled "Back Pain and your Brain" and was recently featured on NPR's All Things Considered.